nature geoscience

Supplementary information https://doi.org/10.1038/s41561-024-01581-4

Long-term carbon storage in shelf sea sediments reduced by intensive bottom trawling

In the format provided by the authors and unedited

Contents

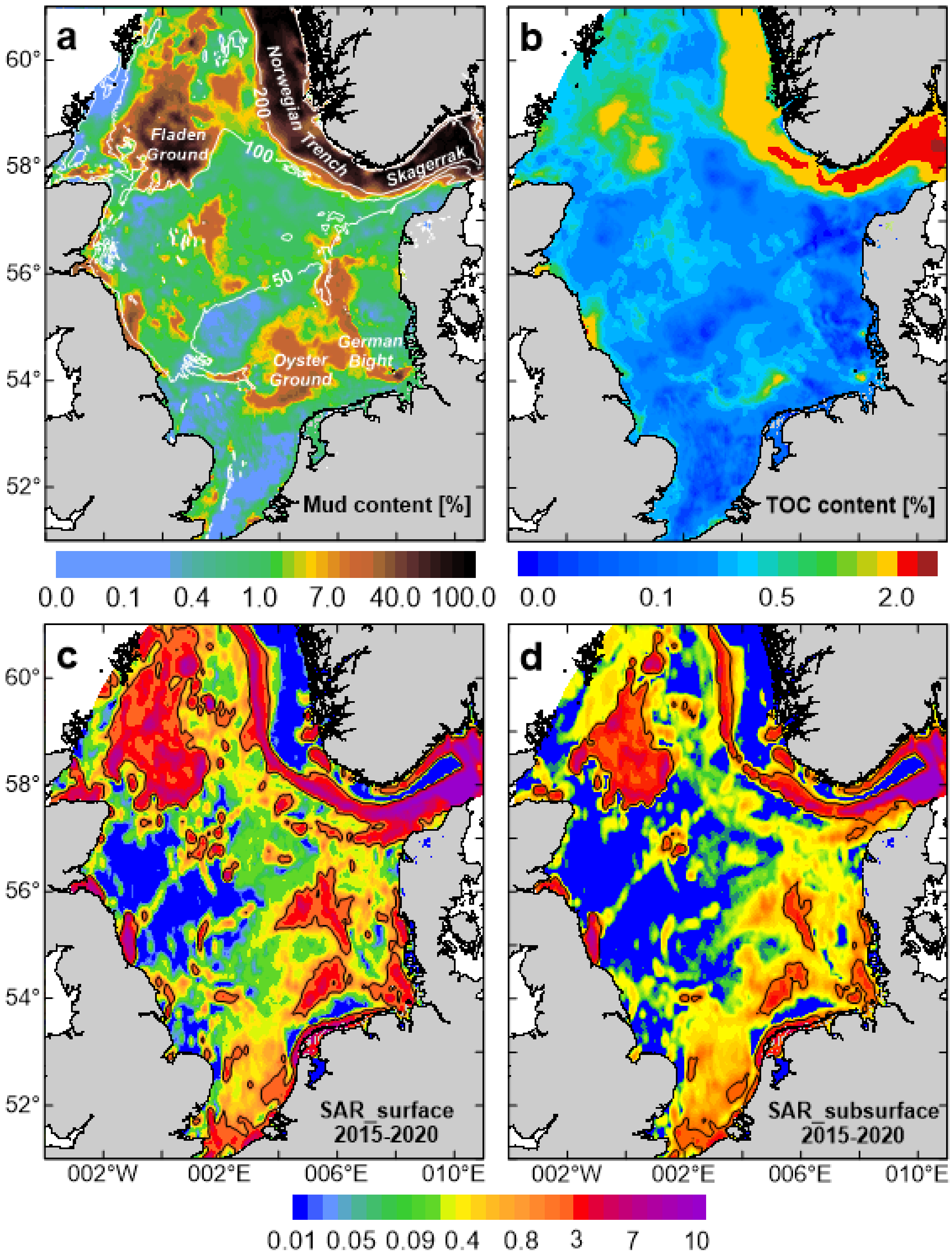

Supplementary Figure 1. Spatial distribution of mud, OC content and bottom trawling intensity in the North Sea. **a,** Mean mud content (%) in the upper 10 cm sediment, with marked large-scale mud depocenters. **b**, Mean Total Organic Carbon (TOC) content (%) in surface 10 cm sediment interpolated from existing field data[48,49]. **c**, Synthesized annual aggregated bottom trawling intensity in terms of swept area ratio (SAR, yr^{-1}) averaged over the period of 2015-2020 in surface sediments (0-2 cm). **d**, similar to (c) but for sub-surface sediments (2-10 cm). The contour line of SAR=1 yr^{-1} is indicated in (c) and (d). All color plots are in logarithmic scale.

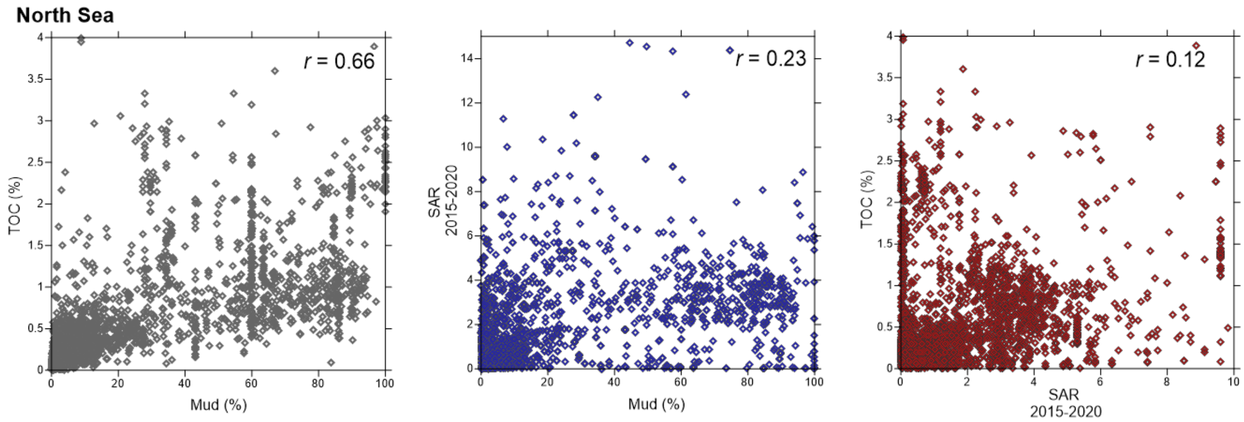

Supplementary Figure 2. Correlation between mud content and OC content, between multi-year (2015-2020) averaged SAR and mud content and between SAR and OC content referred from the North Sea dataset (n = 2380).

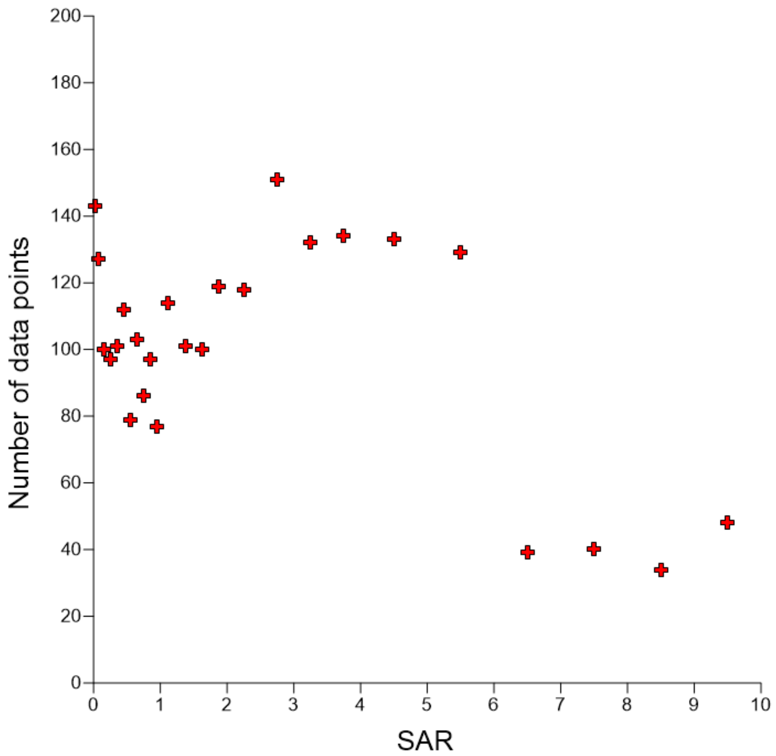

Supplementary Figure 3. Number of field data points in each aggregated interval.

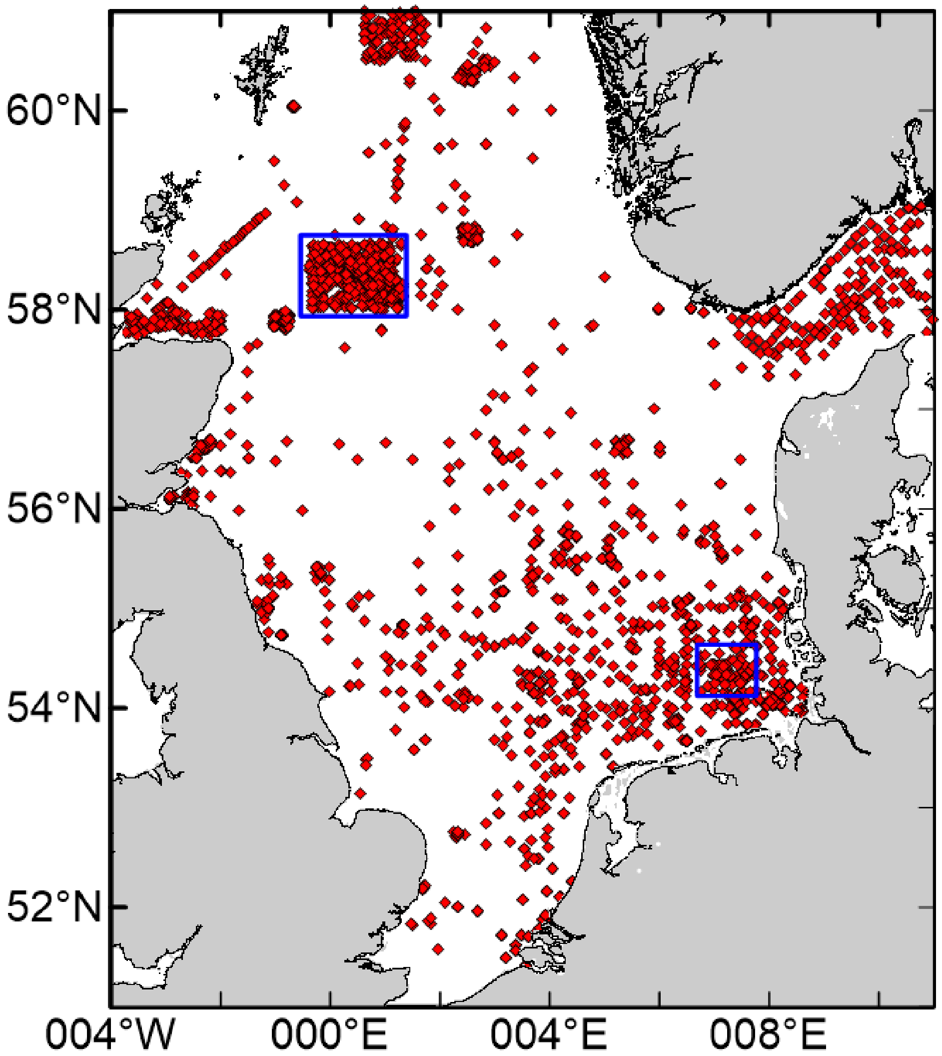

Supplementary Figure 4. Distribution of field sampling stations in the North Sea. Data from two densely sampled local areas (indicated by the rectangles) representing sandy (German Bight, n = 167) and muddy seabed (Fladen Ground, n = 450) are shown in Figure 2 (main text).

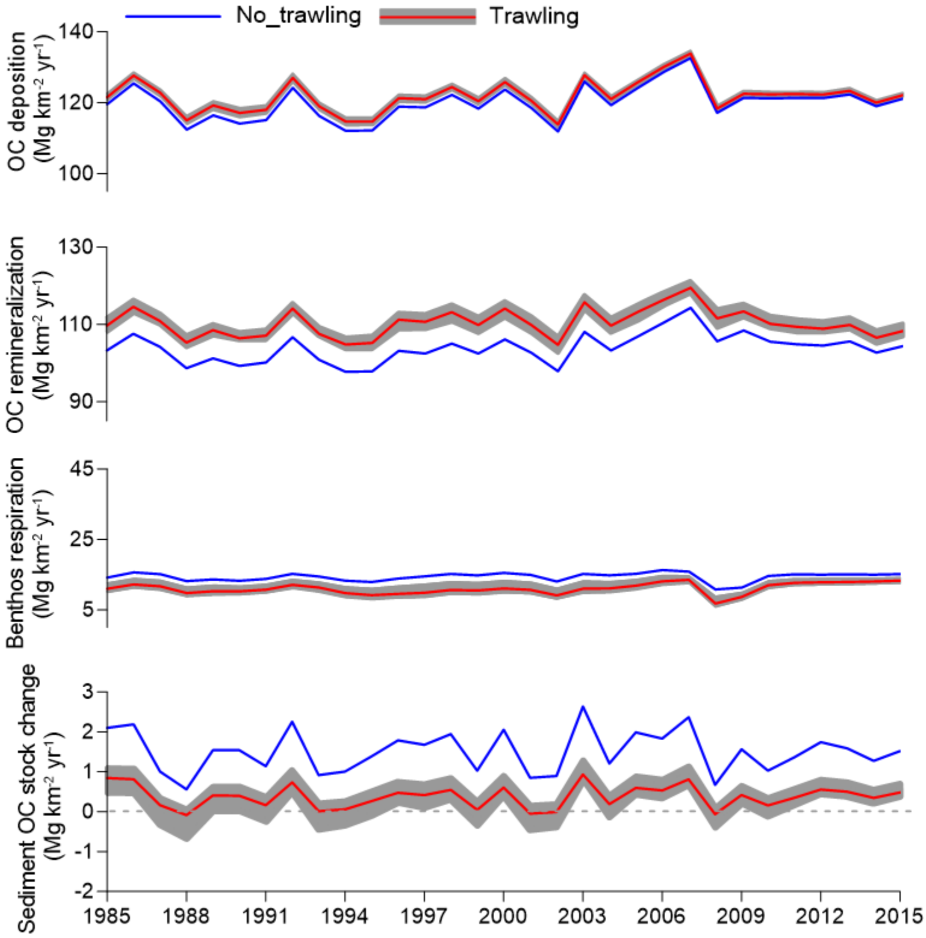

Supplementary Figure 5. Simulated change of the major source and sink terms of sedimentary OC as well as the resultant net stock change in the North Sea. The upper and lower edge of the grey zone for the trawling result refer to the mean ± standard deviation of the model results from the 18 trawling scenarios, respectively. The mean values are indicated by the red curve.

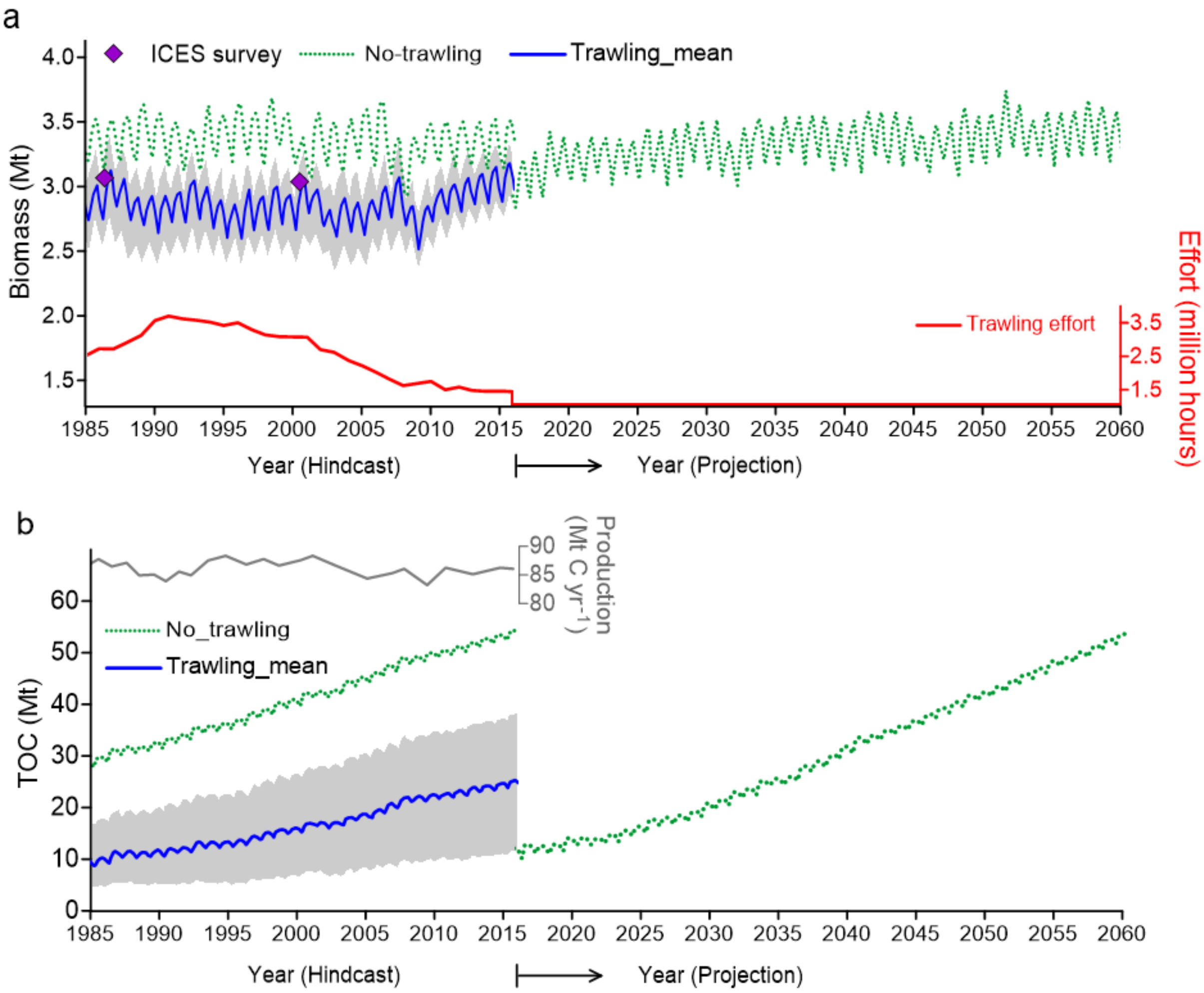

Supplementary Figure 6. Comparison of simulated macrobenthos biomass and OC stock in surface sediments between scenarios with trawling and without trawling (No-Trawling) in the North Sea. The reference of OC stock in (**b**) is the model result after the first-loop of simulation. Annual trawling effort is added in (**a**). Time series of simulated net annual primary production is indicated by the grey line with y-axis on the right in (**b**). The upper and lower edge of the grey zone in (**a**) and (**b**) refer to the mean ± standard deviation of the model results from the 18 trawling scenarios, respectively. The mean values are indicated by the blue curve. Model projection of recovery of macrobenthic biomass and OC stock in the highest trawling impact scenario (Trawling_M3_10pct_phymix1) with trawling stopped is also shown in both plots.

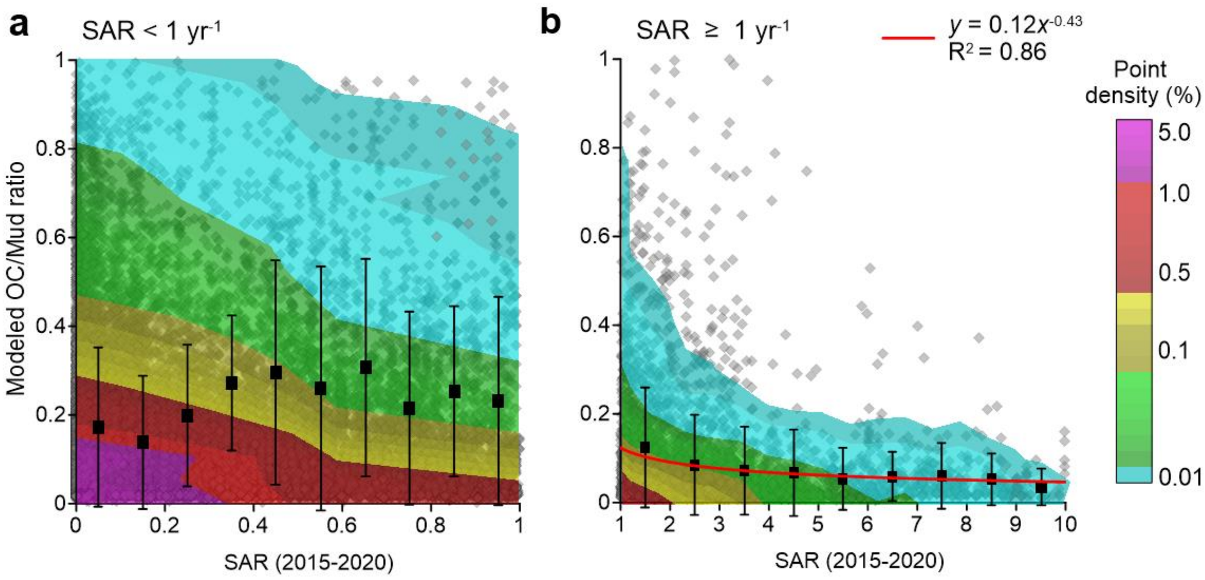

Supplementary Figure 7. **Distribution of modeled OC/mud in relation with the multi-year averaged SAR in the entire North Sea after 50 years' trawling**. **a**, Distribution in weakly or untrawled areas (SAR < 1 yr^{-1}, *n* = 59900). **b**, Similar to (a) but for intensely trawled areas (SAR ≥ 1 yr^{-1}, *n* = 25030). The means ± standard deviations are indicated by dots and error bars.

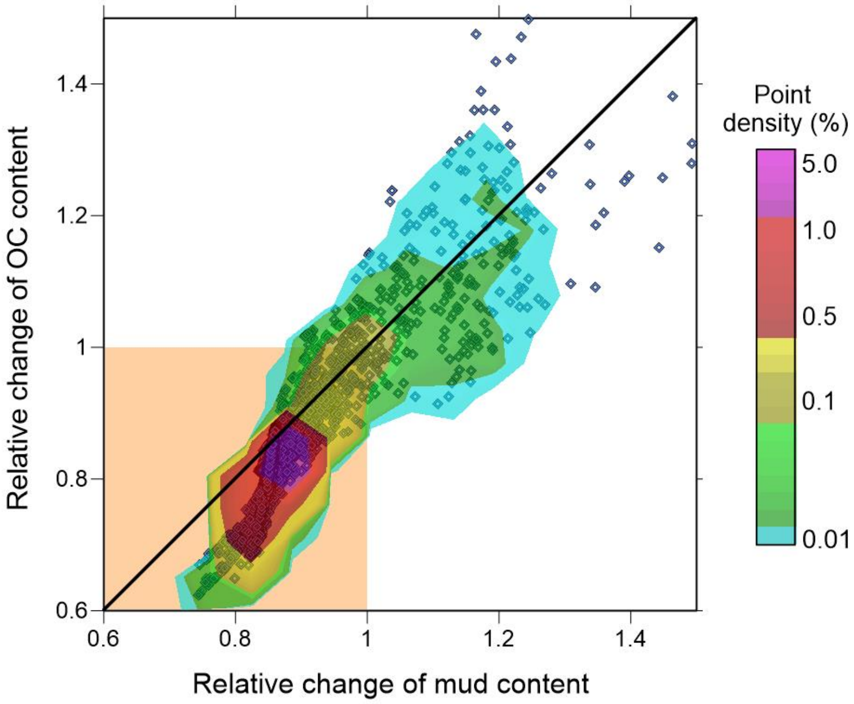

Supplementary Figure 8. Comparison of simulated relative change of mud and OC content in surface sediments of intensively trawled areas (SAR > 1 yr^{-1}) in the North Sea after 50 yrs' trawling. The diagonal line indicates unchanged OC/mud.

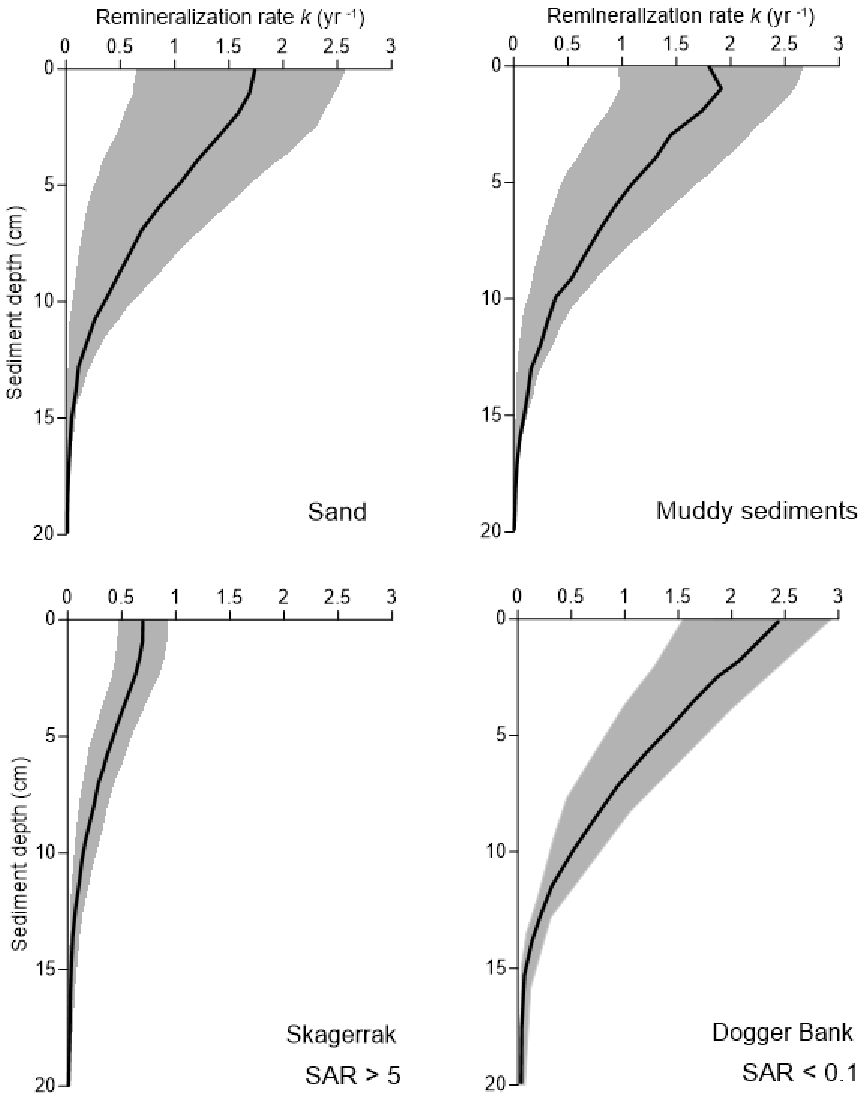

Supplementary Figure 9. Vertical distribution of simulated overall remineralization rate (*k*) of organic carbon in North Sea sediments. The black curves refer to the mean value and the space between the 10th and 90th percentiles is marked by grey colour.

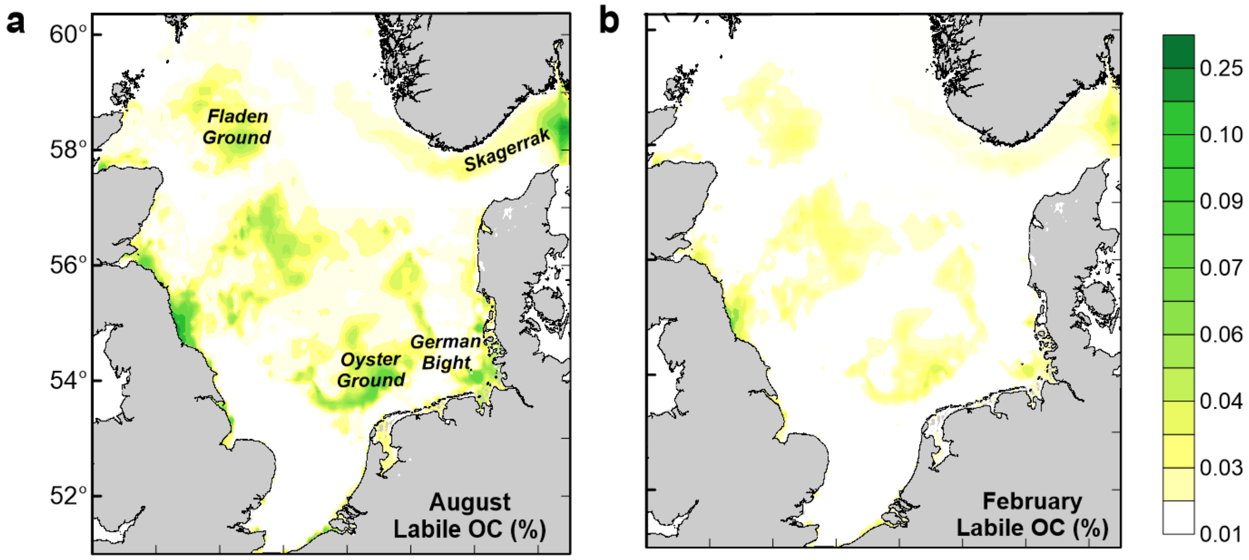

Supplementary Figure 10. Simulated distribution of labile OC content (%) in the North Sea surface sediments (averaged over the upper 10 cm) in summer (a) and winter (b) of the No_trawling scenario.

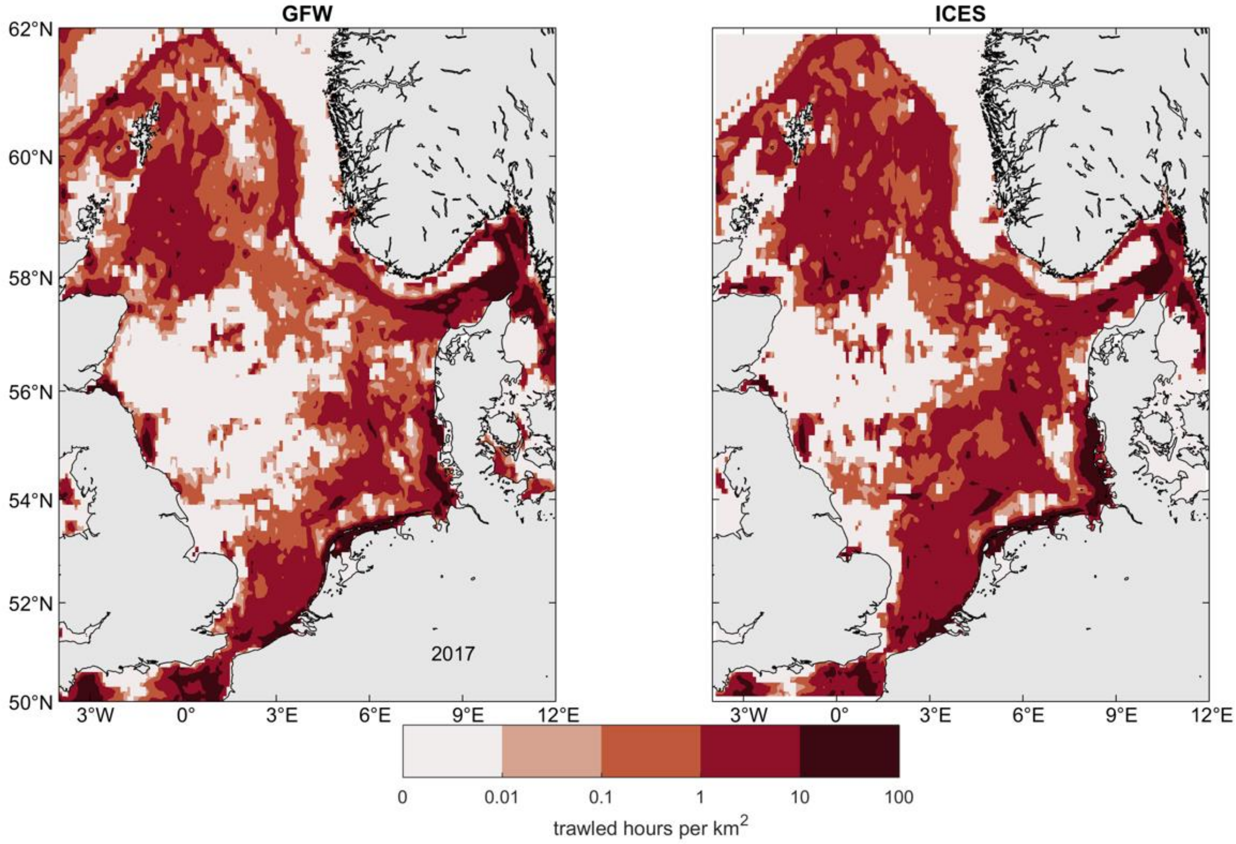

Supplementary Figure 11. **Comparison of multi-year (2015-2020) averaged bottom trawling effort in the North Sea between the daily-resolved AIS dataset[23] and annually aggregated ICES dataset[53].**

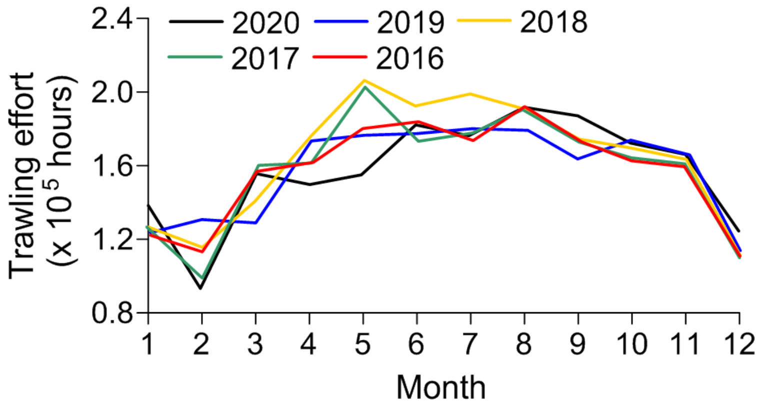

Supplementary Figure 12. Monthly distribution of bottom trawling effort in the North Sea for the period 2016-2020 derived from the daily-resolved AIS dataset[23].

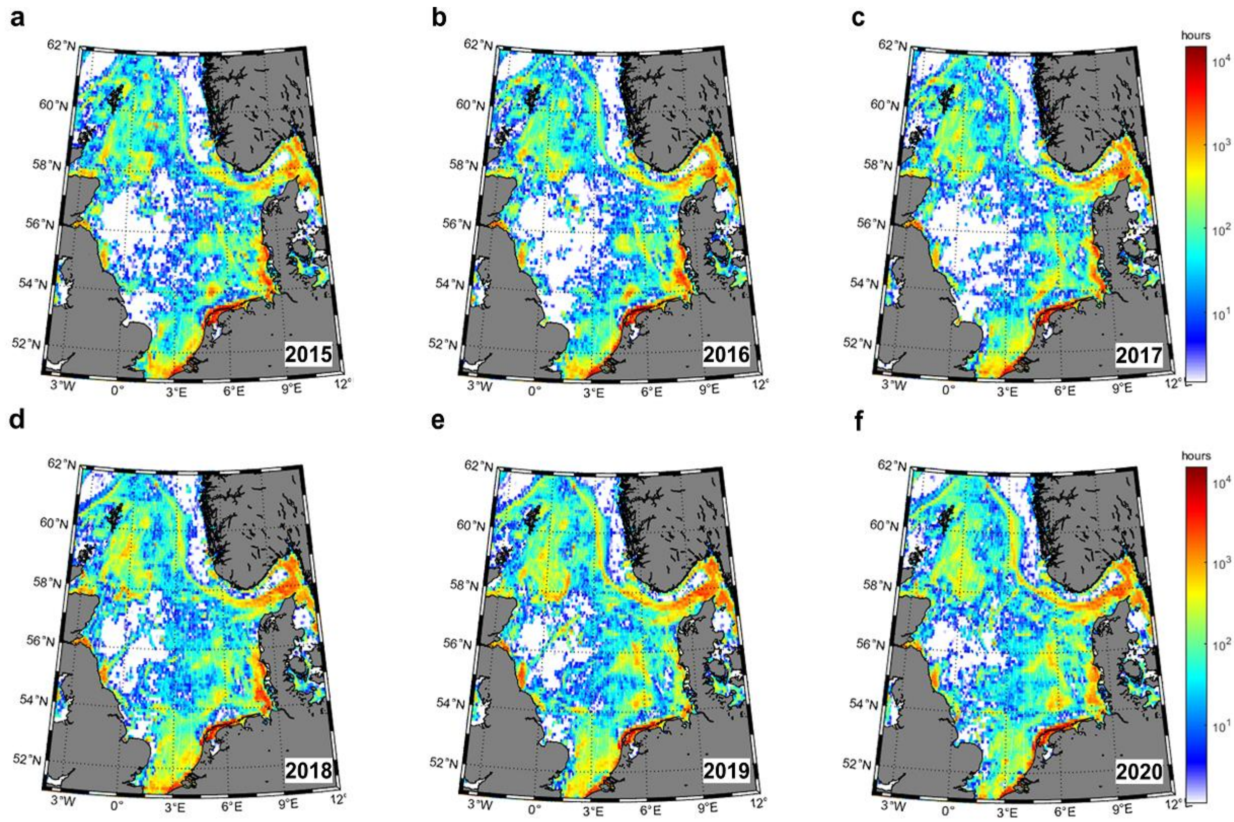

Supplementary Figure 13. Spatial distribution of annual aggregated bottom trawling effort in the North Sea for the period 2015-2020 derived from the daily-resolved AIS dataset[23].

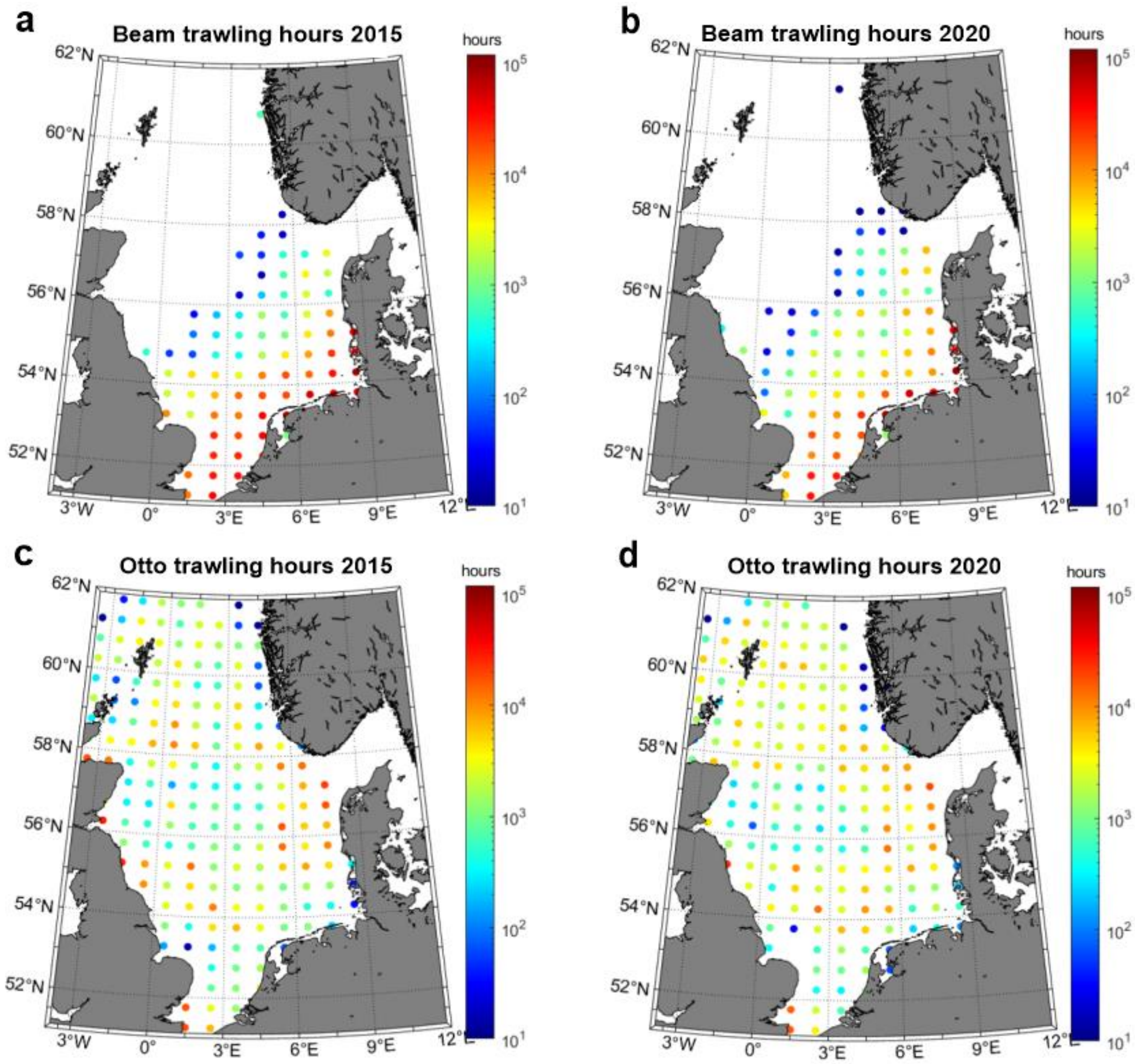

Supplementary Figure 14. Annual aggregated bottom trawling effort by two dominant métiers (beam and otter trawlers) for the year 2015 and 2020 derived from the daily-resolved AIS dataset[23].

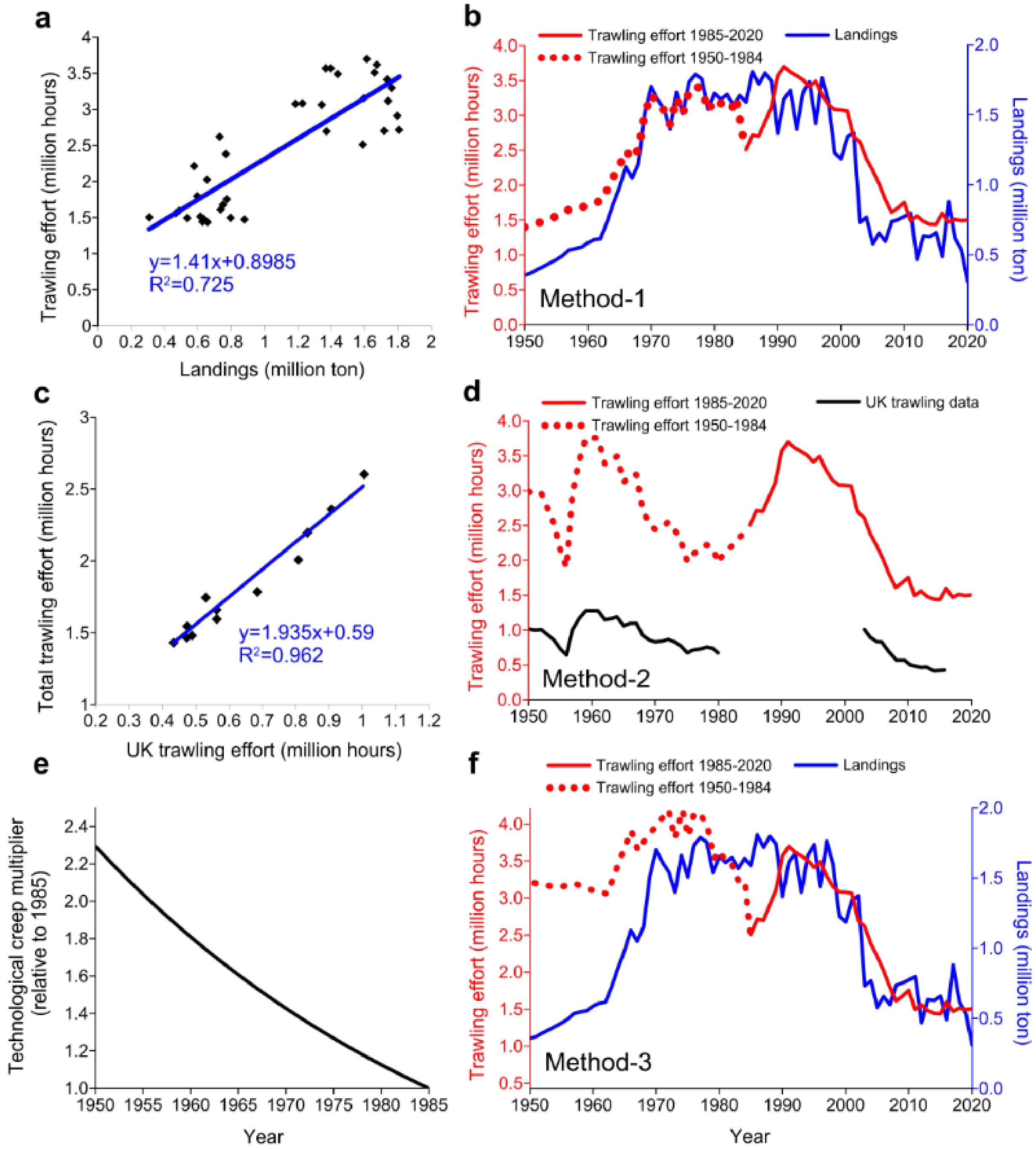

Supplementary Figure 15. Reconstructed time series of annual trawling effort for 1950-1984 using three different scaling methods. **a**, Linear regression analysis between landings and total trawling effort in the North Sea for the period 1985-2020. **b**, Reconstructed total trawling effort (1950-1984) based on the linear regression relationship in (a). **c**, Linear regression analysis between UK trawling effort and total trawling effort in the North Sea for the period 2003-2015. **d**, Reconstructed total trawling effort (1950-1984) based on the linear regression relationship in (c). **e**, Technological creep multiplier in scaling the trawling effort with landings for the period 1950-1984. **f**, Reconstructed total trawling effort (1950-1984) based on the linear regression relationship in (a) with additional increase of technological efficiency. The monitored total trawling effort for 1985-2020 is also shown in (b), (d) and (f).

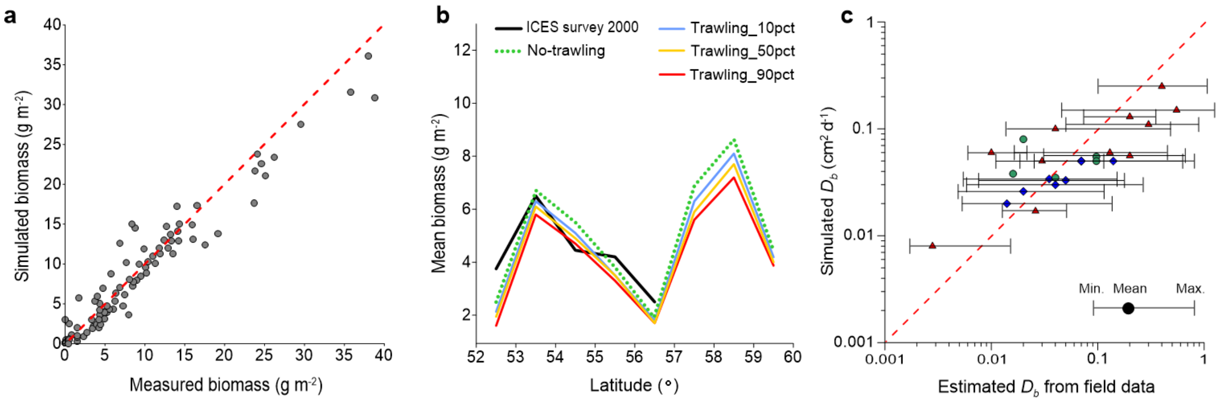

Supplementary Figure 16. Comparison between field-derived and simulated values. a. Macrobenthic biomass at sampling stations (n = 56) with sources listed in Supplementary Table 2. The RMSE is 2.23 g m^{-2}, equivalent to 40% of the spatially averaged value in the entire North Sea. **b**, Mean biomass over each degree in latitude. **c**, Bioturbation rate. Field data sources are distinguished in (c). Red triangles indicate data from the southern North Sea estimated mainly from Chlorophyll profiles (data from this study), green circles are from Solan et al.[70] and blue diamonds (data from this study) are from the northern North Sea estimated mainly from 210Pb profiles. The Normalized RMSE for bioturbation rate is 0.176.

Supplementary Table 1. Numerical experiments representing scenarios of varying impacts of bottom trawling in the study.

Name of scenario	Trawling included	Trawling reconstruction method for 1950-1984	Mortality in macrobenthos scaled by SAR	Physical mixing coefficient scaled by SAR (cm^2 d^{-1})
No_trawling	No			
Trawling_M1_10pct_phymix1	Yes	Method_1	11%	0.24
Trawling_M1_10pct_phymix10	Yes	Method_1	11%	2.4
Trawling_M1_50pct_phymix1	Yes	Method_1	20%	0.24
Trawling_M1_50pct_phymix10	Yes	Method_1	20%	2.4
Trawling_M1_90pct_phymix1	Yes	Method_1	30%	0.24
Trawling_M1_90pct_phymix10	Yes	Method_1	30%	2.4
Trawling_M2_10pct_phymix1	Yes	Method_2	11%	0.24
Trawling_M2_10pct_phymix10	Yes	Method_2	11%	2.4
Trawling_M2_50pct_phymix1	Yes	Method_2	20%	0.24
Trawling_M2_50pct_phymix10	Yes	Method_2	20%	2.4
Trawling_M2_90pct_phymix1	Yes	Method_2	30%	0.24
Trawling_M2_90pct_phymix10	Yes	Method_2	30%	2.4
Trawling_M3_10pct_phymix1	Yes	Method_3	11%	0.24
Trawling_M3_10pct_phymix10	Yes	Method_3	11%	2.4
Trawling_M3_50pct_phymix1	Yes	Method_3	20%	0.24
Trawling_M3_50pct_phymix10	Yes	Method_3	20%	2.4
Trawling_M3_90pct_phymix1	Yes	Method_3	30%	0.24
Trawling_M3_90pct_phymix10	Yes	Method_3	30%	2.4

Supplementary Table 2. Summary of field data in the North Sea

Nr stations	Sampling time (mm/yy)	Data type	Source
6	03/99, 08/00	TOC, mud & Benthos	(1)
15	08/92, 05/93	TOC, mud & Benthos	(2)
35	06-10/21	TOC, mud & Benthos	(3)
2380	1990-2022	TOC & mud	(4)

Note. Sources: (1) Ståhl et al.[72]; (2) Rosenberg et al.[73]; (3) Zhang et al.[29] ;(4) This study.

Supplementary Table 3. Maximum penetration depths of different gear components used in the model. Layers above the maximum impacted depth are considered impacted. Ground gear is separated into a surface and a subsurface component based on the métier using the ratios given in Eigaard et al.[54]

Gear component	Maximum penetration depth (cm)	
	Sand (<10% mud content)	Mud (≥10% mud content)
Otter trawl doors	5	10
Beam trawl shoes	10	10
Sweeps, chains and bridles	2	5
Tickler chains	5	10
Ground gear subsurface	5	10
Ground gear surface	2	2

Supplementary Table 4. Data sources used in this study.

Data description	Reference	URL
Gridded data of surface mud content in the North Sea sediments	Bockelmann, F. D. Mud content of Noarth Sea surface sediments. World Data Center for	https://doi.org/10.1594/WDCC/coastMap_Substrate_Mud

	Climate (WDCC) at DKRZ (2017).	
Gridded data of surface organic carbon content in the North Sea sediments	Bockelmann, F.D. Total organic carbon content of North Sea surface sediments. World Data Center for Climate (WDCC) at DKRZ (2017).	https://doi.org/10.1594/WDCC/coastMap_Substrate_TOC
Global surface mud and OC content	Jenkins, C. Building offshore soils databases. *Sea Technol*. **38**, 25–28 (1997).	https://instaar.colorado.edu/~jenkinsc/dbseabed/
Global surface sediment OC content	Atwood, T. B., Witt, A., Mayorga, J., Hammill, E. & Sala, E. Global Patterns in Marine Sediment Carbon Stocks. *Front. Mar. Sci*. **7**, 165 (2020).	https://figshare.com/articles/marine_soil_carbon/9941816
Global annual surface sediment SAR	Kroodsma, D.A. et al. Tracking the global footprint of fisheries. *Science* **359**, 904–908 (2018).	https://globalfishingwatch.org/datasets-and-code/

Annual aggregated bottom trawling effort from the ICES data	ICES. OSPAR request 2018 for spatial data layers of fishing intensity/pressure. Data Outputs (2019).	https://doi.org/10.17895/ices.data.4686
Field and model data of OC and macrobenthos	Zhang, W. Field and Model Data for Bottom Trawling Impacts in the North Sea (Version 1) (2023).	https://doi.org/10.5281/zenodo.8297751
Daily aggregated spatial data on bottom trawling in the North Sea for the period 2015-2020	Zhang, W. Field and Model Data for Bottom Trawling Impacts in the North Sea (Version 1) (2023).	https://doi.org/10.5281/zenodo.8297751
Multi-year averaged surface sediment swept area ratio (SAR 2015-2020)	Zhang, W. Field and Model Data for Bottom Trawling Impacts in the North Sea (Version 1) (2023).	https://doi.org/10.5281/zenodo.8297751

Model code and simulation results	Zhang, W. Field and Model Data for Bottom Trawling Impacts in the North Sea (Version 1) (2023).	https://doi.org/10.5281/zenodo.8297751
Annual aggregated trawling-induced resuspension rate in the North Sea 2015-2020	Zhang, W. Field and Model Data for Bottom Trawling Impacts in the North Sea (Version 1) (2023).	https://doi.org/10.5281/zenodo.8297751
Point data and R code	Zhang, W. Point data and R code for multivariate analysis of Bottom Trawling Impacts in the North Sea (Version 1) (2023).	https://doi.org/10.5281/zenodo.13322571

Supplementary Text 1. Regression analysis using Instrumental Variables

The instrumental variable (IV) approach isolates the exogenous variation of the explanatory variable to estimate its causal effect on the dependent variable[75]. In our case, water depth is used as an instrument for SAR. Specifically, a binary depth dummy variable with a cutoff at 150 m is created, based on the observation that fishing activities significantly decrease beyond this depth (see Supplementary Supplementary Figure ***1***6). Therefore, $depth$ is converted to a binary variable which is equal to 0 if $depth$ is smaller than 150 m and 1 otherwise:

$$depth\_dummy_i = \begin{cases} 1 \; if \; depth_i \geq \; 150 \text{ m} \\ 0 \; if \; depth_i < \; 150 \text{ m} \end{cases}$$

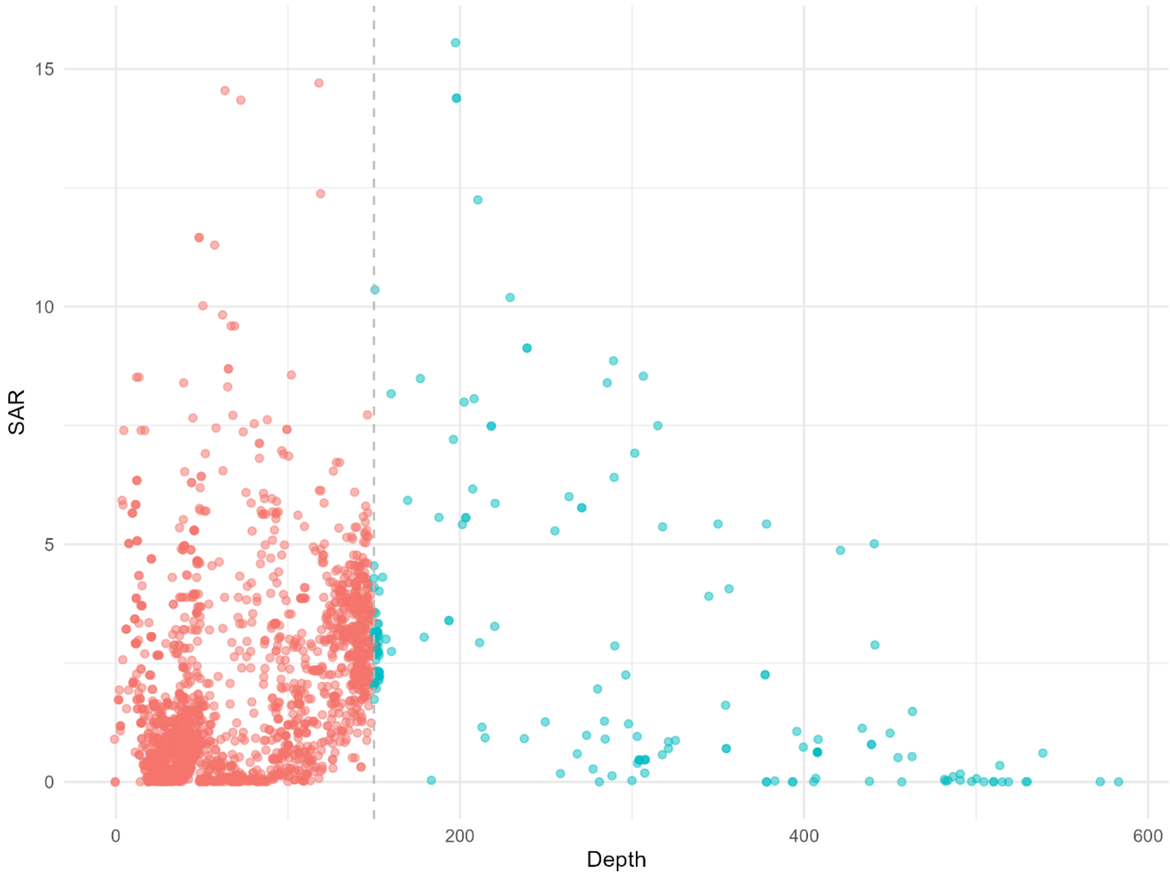

Supplementary Figure 17. SAR versus depth (m). The dashed line at 150 m indicates the cut-off point for the instrument which is used in the regression analysis.

The IV approach proceeds in two stages: In the first stage, SAR is regressed on $depth\_dummy$ and the other covariates (*mud*, *tau*, *dist*, *phy*, *temp*) to obtain the estimated predicted values $\widehat{SAR}_i$:

$$\widehat{SAR}_i = \alpha_0 + \alpha_1 \cdot depth\_dummy_i + \alpha_2 \cdot mud_i + \alpha_3 \cdot tau_i + \alpha_4 \cdot dist_i + \alpha_5 \cdot phy_i + \alpha_6 \cdot temp_i + \varepsilon_i,$$

with coefficients α_0 to α_6 and error term ε_i.

In the second stage, OC is regressed on the obtained values $\widehat{SAR}_i$ and the same covariates to estimate the treatment effect:

$$OC_i = \beta_0 + \beta_1 \cdot \widehat{SAR}_i + \beta_2 \cdot mud_i + \beta_3 \cdot tau_i + \beta_4 \cdot dist_i + \beta_5 \cdot phy_i + \beta_6 \cdot temp_i + \vartheta_i,$$

with coefficients β_0 to β_6 and error term ϑ_i.

In the first stage of the IV regression, the F-statistic indicates how well the instrument variables explain the endogenous variable. A high F-statistic result (typically above 10) in the first stage suggests that the instrument variable ($depth\_dummy$) is well-suited to explain the endogenous variable. In our case, the F-statistic of 81.25 indicates that the instrument variable is a strong instrument for estimating SAR. The 'Kleibergen-Paap rk Wald F'-statistic of 13.55 indicates that the instrument used is strong and relevant, addressing the potential endogeneity of SAR[76].

Regression results are provided in Supplementary Supplementary Table . The statistical model shows a highly significant (p<0.05) negative effect of SAR on OC when all relevant covariates are included. The sign of the effect is consistent with the OLS regression, but the effect size of SAR is increased in the IV approach, suggesting that the instrumented values of SAR overestimate the negative impact on OC.

Supplementary Table 5. Results of the multivariate linear regression on OC using the IV approach. Robust standard errors are in parentheses. Three outliers identified by Cook's Distance were removed. The p-values are based on two-sided tests. No adjustments were made for multiple comparisons. Kleibergen-Paap rk Wald F statistic: 13.55; First-stage F-statistic: 81.25. ***p<0.01, **p<0.05, *p<0.1.

Variables	**Reg. 1**	**Reg. 2**	**Reg. 3**	**Reg. 4**	**Reg. 5**
SAR	-1.856 (1.2592)	-1.4987* (0.8182)	-0.9968** (0.4058)	-1.0515** (0.4694)	-0.943** (0.3766)
Mud (%)	0.0584* (0.0315)	0.0535** (0.0226)	0.0414*** (0.0117)	0.0441*** (0.0143)	0.0368*** (0.0102)
Tau (Pa)		1.3235 (1.6266)	-1.3175 (1.1127)	-2.5619 (1.7846)	-2.0884 (1.5168)
Dist (km)			-0.004*** (0.0012)	-0.0037*** (0.0011)	-0.0042*** (0.0011)
Phy (mg/m³)				0.0041 (0.0037)	0.0134** (0.0063)
Temp (°C)					-0.2255*** (0.0832)
SAR (95% CI Lower)	-4.3252	-3.1033	-1.7926	-1.9721	-1.6816
SAR (95% CI Upper)	0.6131	0.1059	-0.201	-0.1309	-0.2044
Kleibergen-Paap rk Wald F statistic	5.09	7.8928	13.481	11.2826	13.5526
First-stage F-statistic	187.2627	139.0133	110.1923	91.0809	81.2519

Reference

73. Ståhl, H. et al. Factors influencing organic carbon recycling and burial in Skagerrak sediments. *J. Mar. Res.* **62,** 867-907 (2004).
74. Rosenberg, R., Hellman, B., & Lundberg, A. Benthic macrofaunal community structure in the Norwegian Trench, deep skaggerrak. *J. Sea Res.* **35 (1-3)**, 181-188 (1996).
75. Angrist, J.D., Imbens, G.W., Rubin, D.B. Identification of Causal Effects Using Instrumental Variables. *Journal of the American Statistical Association* **91**, 444–455 (1996).
76. Kleibergen, F., Paap, R. Generalized reduced rank tests using the singular value decomposition. *Journal of Econometrics* **133**, 97–126 (2006).